382

A finite-element scheme for the vertical discretization in the semi-Lagrangian version of the ECMWF forecast model

A. Untch and M. Hortal

Research Department

April 2003

For additional copies please contact

The Library
ECMWF
Shinfield Park
Reading, Berks RG2 9AX

library@ecmwf.int

Series: ECMWF Technical Memoranda

A full list of ECMWF Publications can be found on our web site under:
http://www.ecmwf.int/publications.html

Abstract

A vertical finite-element discretization designed for the ECMWF model with semi-Lagrangian advection is described. Only non-local operations are evaluated in finite-element representation, while products of variables are evaluated in physical space. With semi-Lagrangian advection, the only non-local vertical operations to be evaluated are vertical integrals. An integral operator is derived based on the Galerkin method using B-splines as basis functions with compact support. Two versions have been implemented, one using piecewise linear basis functions (hat functions) and the other using cubic B-splines. No staggering of dependent variables is employed in physical space, making the method well suited for use with semi-Lagrangian advection.

The two versions of the finite-element scheme are compared to finite-difference schemes in both the Lorenz and the Charney-Phillips staggering of the dependent variables for the linearized model. The finite-element schemes give more accurate results than the two finite-difference schemes for the phase speeds of most of the linear gravity waves. We show evidence that the finite-element schemes suffer less from the computational mode than the finite-difference scheme with Lorenz staggering, although temperature and geopotential are held at the same set of levels in the finite-element scheme too. As a result, the finite-element schemes reduce the level of vertical noise in forecasts with the full model. They also reduce by about 50% a persistent cold bias in the lower stratosphere present with the finite-difference scheme in Lorenz staggering (i.e. the operational scheme at ECMWF before its recent replacement by the cubic version of the finite- element scheme described here) and improves the transport in the stratosphere.

1. Introduction

We describe a finite-element (FE) scheme for the vertical discretization of the ECMWF model. This scheme was implemented in the operational model version CY24R3 in January 2002.

The vertical discretization in the ECMWF model had not changed significantly from the finite- difference (FD) scheme of Simmons and Burridge (1981), except for the introduction of the semi- Lagrangian scheme for the vertical advection (*Ritchie et al.*, 1995). This vertical FD scheme uses Lorenz staggering of the dependent variables (*Lorenz*, 1960) and is only first order accurate for non-uniform spacing of levels.

The finite-element method constitutes a very attractive method for constructing an accurate vertical discretization, since it is a Galerkin type method which uses as basis functions piecewise continuous functions with compact support (only locally non-zero) instead of globally defined functions, as in spectral methods. Finding suitable, globally defined, orthogonal polynomials as basis functions for the vertical of primitive equations models has proven difficult (*Machenhauer and Daley*, 1972; *Francis*, 1972; *Hoskins*, 1973). Polynomial functions with compact support constitute a good alternative and allow for great flexibility in dealing with boundary conditions.

Finite-element based discretizations for the vertical have been tried successfully in several atmospheric models (*Staniforth and Daley*, 1977; *Burridge et al*., 1986; *Steppeler*, 1987). However, an earlier attempt to replace the Simmons and Burridge FD scheme in the operational version of the ECMWF model by a finite-element scheme (*Steppeler*, 1987) was unsuccessful because of numerical instability.

The vertical finite-element scheme developed here is designed to be used with semi-Lagrangian advection. For this reason, we do not employ any staggering of dependent variables, so all fields (even vertical velocity) are carried on the same set of levels as in *Staniforth and Daley* (1977) and *Steppeler* (1987). Holding the horizontal winds and the temperature on staggered sets of levels as in Charney-Phillips arrangement

(*Charney and Phillips*, 1953) has advantages for treating the gravity wave terms of the forecast equations but causes difficulties for semi-Lagrangian advection. In contrast, holding the horizontal winds and temperature at the same set of levels as in Lorenz arrangement gives rise to a computational (zigzag) mode in the vertical distribution of temperature (*Tokioka*, 1978; *Hollingsworth*, 1995; *Arakawa and Konor*, 1996). We show evidence in this paper that this computational mode is damped by the FE discretization compared to the FD discretization.

We execute only non-local vertical operations in finite-element space and evaluate products of dependent variables (and of course, the semi-Lagrangian advection) in physical space. This is analogous to the spectral transform method used for the horizontal (*Ritchie et al.*, 1995). With semi-Lagrangian vertical advection, the only non-local vertical operations to be evaluated are vertical integrals, since we use the continuity and the hydrostatic equations in integrated form. We derive an "integral operator" in FE representation by using the Galerkin method and B-splines as basis functions with compact support. The scheme can, in principle, use piecewise continuous polynomials of any degree with compact support as basis functions. We have implemented and tested it with linear elements (linear FE scheme) and with cubic spline elements (cubic FE scheme).

After reviewing the hydrostatic forecast equations in the form used at ECMWF in section 2, we describe the derivation of the FE integral operators with linear and cubic elements in section 3 and estimate their order of accuracy when applied to the integration of a smooth function. In section 4 we show the impact of the FE schemes on the forecast model, beginning with the linearized model and compare with the FD schemes in Lorenz and in Charney-Phillips staggering of variables. We then present results from extensive assimilation-forecast experiments with the cubic FE scheme, selected as the more accurate scheme for operational implementation. Finally, a summary of the results and discussion are given in section 5.

2. Governing equations

The evolution equations used in the semi-Lagrangian version of the ECMWF forecast model are (*Ritchie et al.*, 1995):

momentum equation

$$\frac{d\vec{V}_H}{dt} + f\vec{k}\times\vec{V}_H + \nabla_H\Phi + R_d T_V \nabla_H \ln p = P_V + K_V \tag{2.1}$$

thermodynamic equation

$$\frac{dT}{dt} - \frac{\kappa T_V \omega}{(1+(\delta-1)Q)\,p} = P_T + K_T \tag{2.2}$$

continuity equation

$$\frac{\partial}{\partial t}\left(\frac{\partial p}{d\eta}\right) + \nabla_H \bullet \left(\vec{V}_H \frac{\partial p}{\partial \eta}\right) + \frac{\partial}{\partial \eta}\left(\dot{\eta}\frac{\partial p}{\partial \eta}\right) = 0 \tag{2.3}$$

humidity equation

$$\frac{dQ}{dt} = P_Q \tag{2.4}$$

and **hydrostatic equation**

$$\nabla_H \Phi = \nabla_H \Phi_S + \nabla_H \int_1^\eta (-R_d T_V \frac{\partial}{\partial \eta'} (\ln p)) d\eta' \tag{2.5}$$

Here $\vec{V}_H$ denotes the "horizontal" velocity, ∇_H the horizontal gradient operator, f the Coriolis parameter, T_V virtual temperature, Φ_S surface geopotential, η the (pressure-based) hybrid vertical coordinate (*Simmons and Strüffing*, 1983), ω the "pressure" vertical velocity (dp/dt), $\kappa = R_d / C_{pd}$, $\delta = C_{pv} / C_{pd}$ and P and K the physical parametrization and the horizontal diffusion contributions, respectively. All other notations follow standard conventions.

The hybrid vertical coordinate $\eta(p, p_s)$ is a monotonic function of pressure and also depends on surface pressure such that $\eta = 1$ for $p = p_s$ and $\eta = 0$ for $p = 0$. Pressure as a function of η is given by

$$p(\eta) = A(\eta) + B(\eta) \cdot p_s \tag{2.6}$$

where the functions $A(\eta)$ and $B(\eta)$ have to fulfil the conditions

$$A(1) = 0, \quad B(1) = 1, \quad A(0) = B(0) = 0 \tag{2.7}$$

which ensure that $p(1) = p_s$ and $p(0) = 0$. An equivalent definition of the vertical coordinate, but one better suited for the construction of the finite-element based discretization for the vertical with no staggering of variables presented here, is given by the derivative form of (2.6)

$$\frac{\partial p}{\partial \eta} = \frac{dA}{d\eta} + \frac{dB}{d\eta} p_s \tag{2.8}$$

together with the conditions

$$\int_0^1 \frac{dA}{d\eta} d\eta = 0, \quad \int_0^1 \frac{dB}{d\eta} d\eta = 1 \tag{2.9}$$

which ensure that the integral of pressure from the top of the atmosphere to the surface yields the surface pressure p_s.

By integrating the continuity equation in the vertical subject to the boundary conditions $\dot{\eta} = 0$ at $\eta = 1$ and at $\eta = 0$, we obtain expressions for the vertical velocity ω, for $\dot{\eta} \equiv \frac{d\eta}{dt}$, and for the rate of change of surface pressure

$$\omega = -\int_0^\eta \left(\frac{\partial p}{\partial \eta'} D + \frac{dB}{d\eta'} \vec{V}_H \cdot \nabla_H p_s \right) d\eta' + B \vec{V}_H \cdot \nabla_H p_s \tag{2.10}$$

$$\dot{\eta} \frac{\partial p}{\partial \eta} = -\frac{\partial p}{\partial t} - \int_0^\eta \nabla_H \cdot (\vec{V}_H \frac{\partial p}{\partial \eta'}) d\eta' \tag{2.11}$$

$$\frac{\partial}{\partial t}(\ln p_s) = -\frac{1}{p_s}\int_0^1 \nabla_H \cdot (\vec{V}_H \frac{\partial p}{\partial \eta})d\eta = -\frac{1}{p_s}\int_0^1 \left(D\frac{\partial p}{\partial \eta} + \frac{dB}{d\eta}\vec{V}_H \cdot \nabla_H p_s \right) d\eta \qquad (2.12)$$

Here D is horizontal divergence.

For the semi-Lagrangian advection scheme an expression for the total time derivative of surface pressure is required:

$$\frac{d}{dt}(\ln p_s) = \int_0^1 \left(\frac{dB}{d\eta}\frac{\partial}{\partial t}(\ln p_s) + \frac{dB}{d\eta}\vec{V}_H \cdot \nabla_H \ln p_s \right) d\eta \qquad (2.13)$$

where $\partial(\ln p_s)/(\partial t)$ is given by (2.12) above.

3. Finite-element scheme

3.1 Vertical discretization

In the Simmons & Burridge (1981) vertical discretization used operationally at ECMWF until Jan. 2002 when the present finite-element scheme was implemented, the atmosphere (from the surface to p=0) is divided into N layers defined by the interface pressures, referred to as half levels. (The list of half levels includes the top of the atmosphere (p=0) and the surface, too.) The prognostic variables (with the exception of the surface pressure) are represented by their values at full level pressures (which in the model are defined as the average pressure between the adjacent half levels), while the diagnostic quantities such as ω and Φ are kept at the half levels, i.e. a Lorenz arrangement of dependent variables (*Lorenz*, 1960) is used. Vertical derivatives are computed by means of centered finite-difference algorithms and vertical integrals are performed by means of the mid-point rule. We refer to this scheme as the finite-difference (FD) scheme or FD_Lorenz scheme, where we need to distinguish it from a FD scheme with Charney-Phillips staggering of variables.

The values of full level pressures are not explicitly needed in the FD scheme (see *Simmons and Burridge* (1981) for details). Only the values of the half level pressures are required and these are defined by

$$p_{k+1/2} = A_{k+1/2} + B_{k+1/2} \cdot p_s, \quad for \quad 0 \le k \le N \qquad (3.1)$$

where $A_{k+1/2}$ and $B_{k+1/2}$ are specified constants with $A_{1/2} = 0, \quad B_{1/2} = 0$ and $A_{N+1/2} = 0, \quad B_{N+1/2} = 1$ in order to fulfil conditions (2.7).

The values of the vertical coordinate η at full or half level positions were not explicitly required by the FD discretization with Eulerian advection (*Simmons and Burridge* (1981)) but have to be specified for the semi-Lagrangian scheme (*Ritchie et al*, 1995). The η-values at full levels are also needed for the finite-element discretization. The following formal definition of η is used

$$\eta_{k+1/2} = A_{k+1/2} / p_0 + B_{k+1/2}, \quad 0 \le k \le N \qquad (3.2)$$

where p_0 is a constant pressure chosen to be 1013.25 hPa. At full levels, the values of η are given by

$$\eta_k = 0.5(\eta_{k-1/2} + \eta_{k+1/2}) \quad for \quad 1 \le k \le N \qquad (3.3)$$

In the finite-element discretization we keep all variables - including pressure - at the same set of levels (at full levels), i.e. no staggering of variables is used. It is therefore convenient to use definition (2.8) of the vertical coordinate and prescribe $\left(\frac{dA}{d\eta}\right)_k$ and $\left(\frac{dB}{d\eta}\right)_k$ at full levels (instead of $A_{k+1/2}$ and $B_{k+1/2}$ at half levels) such that

$$\left(\frac{\partial p}{\partial \eta}\right)_k = \left(\frac{dA}{d\eta}\right)_k + \left(\frac{dB}{d\eta}\right)_k p_s \tag{3.4}$$

together with the conditions (2.9). These conditions have to be fulfilled to a good approximation with the *numerical integration scheme used in the vertical discretization*. The required pressures at full levels can then be obtained by integrating (3.4) over η from the top of the atmosphere to the full levels.

In the semi-Lagrangian version of the evolution equations in the form given in sect. 2, $\frac{dB}{d\eta}$ and $\frac{\partial p}{\partial \eta}$ are the only vertical derivatives. Since the vertical derivative of pressure can be expressed according to (3.4) in terms of the vertical derivatives of *A* and *B*, which are constant in time and prescribed, only vertical integrals remain to be evaluated.

We now derive a vertical integral operator based on a finite-element representation.

3.2 Vertical integral operator in finite-element representation

The majority of the vertical integrals to evaluate, are integrals from the top of the atmosphere to the individual model levels and to the surface. We therefore derive an operator in finite-element representation for this type of integral, i.e. an operator which returns the integral from the top of the atmosphere to each of the model levels η_k and to the surface $\eta = 1$. The vertical integral in the hydrostatic equation (i.e. from the surface upwards) can be constructed by taking the difference of the integral from the top of the atmosphere to the model level in question minus the integral from the top to the surface.

Let $\{d_i(\eta)\}_{i=K_1}^{K_2}$ and $\{e_i(\eta)\}_{i=M_1}^{M_2}$ be two complete sets of linearly independent functions of compact support which can be used as basis functions to expand any function of the vertical coordinate η given in the domain [0,1].

The vertical integral

$$F(\eta) = \int_0^\eta f(x)dx \tag{3.5}$$

can then be approximated as

$$\sum_{i=K_1}^{K_2} C_i d_i(\eta) = \sum_{i=M_1}^{M_2} c_i \int_0^\eta e_i(x)dx \tag{3.6}$$

where C_i are the coefficients of the expansion of $F(\eta)$ as a linear combination of the basis functions $d_i(\eta)$ and c_i are the coefficients of the expansion of $f(\eta)$ as a linear combination of the basis functions $e_i(\eta)$.

We can then apply the Galerkin procedure to (3.6) by multiplying both sides of this equation by each function from a complete set of "test functions" $\{t_j(\eta)\}_{j=N_1}^{N_2}$ and integrating over the vertical domain:

$$\sum_{i=K_1}^{K_2} C_i \int_0^1 d_i(x) t_j(x) dx = \sum_{i=M_1}^{M_2} c_i \int_0^1 \left(t_j(x) \int_0^x e_i(y)\, dy \right) dx \qquad \text{for } N_1 \le j \le N_2 \tag{3.7}$$

In matrix form this can be expressed as $\underline{\underline{A}}\vec{C} = \underline{\underline{B}}\vec{c} \Rightarrow \vec{C} = \underline{\underline{A}}^{-1}\underline{\underline{B}}\vec{c}$, provided the inverse of $\underline{\underline{A}}$ exists. For the choice of basis and test functions we make in section 3.3 this is the case.

Incorporating into the above expression also the transformations from physical space to finite-element space and back, i.e. $\vec{c} = \underline{\underline{S}}^{-1}\vec{f}$ and $\vec{F} = \underline{\underline{P}}\vec{C}$, we obtain $\vec{F} = \underline{\underline{P}}\,\underline{\underline{A}}^{-1}\underline{\underline{B}}\,\underline{\underline{S}}^{-1}\vec{f} \equiv \underline{\underline{I}}\,\vec{f}$. Here $\vec{f}$ and $\vec{F}$ denote vectors in physical space composed of the values of f and F, respectively, at the model levels: $f_i = f(\eta_i), \quad F_i = F(\eta_i), \quad 1 \le i \le N$. $\vec{F}$ also includes the value of the integral at the surface of the model. These vectors may include values of the first and higher order derivatives of f and F at the boundaries when higher order than linear spline functions are chosen as basis and/or test functions. Details are given in section 3.3 where it is also shown how to compute the projection matrices $\underline{\underline{S}}$ and $\underline{\underline{P}}$ for linear and cubic finite elements.

The matrix $\underline{\underline{I}} \equiv \underline{\underline{P}}\,\underline{\underline{A}}^{-1}\underline{\underline{B}}\,\underline{\underline{S}}^{-1}$ is the integration operator in finite-element formulation which, applied to a function given at full model levels, yields the integrals of this function from the top of the atmosphere to each individual full model level and to the surface.

3.3 Choice of basis functions

The finite-element method outlined above has been implemented in two versions, one based on linear splines (hat functions) (Fig. 1) and the other based on cubic B-splines (*Prenter*, 1975) (Fig. 2). Although in Fig. 1 and Fig. 2 the basis functions are shown for a regular spacing of the model levels, both versions have been implemented for arbitrary level spacing.

A hat function centred around level η_i is simply given by

$$e_i(\eta) = \begin{cases} (\eta - \eta_{i-1})/(\eta_i - \eta_{i-1}) & \text{for} \quad \eta_{i-1} \le \eta \le \eta_i \\ (\eta_{i+1} - \eta)/(\eta_{i+1} - \eta_i) & \text{for} \quad \eta_i \le \eta \le \eta_{i+1} \\ 0 & \text{otherwise} \end{cases} \tag{3.8}$$

The equivalent cubic B-spline covers four intervals around η_i, and an analytic expression for a regular spacing of levels is given by (*Prenter*, 1975, P. 79)

$$B_i(\eta)=\frac{1}{4h^3}\begin{cases}(\eta-\eta_{i-2})^3 & for \quad \eta_{i-2}\le\eta\le\eta_{i-1}\\ h^3+3h^2(\eta-\eta_{i-1})+3h(\eta-\eta_{i-1})^2-3(\eta-\eta_{i-1})^3 & for \quad \eta_{i-1}\le\eta\le\eta_{i}\\ h^3+3h^2(\eta_{i+1}-\eta)+3h(\eta_{i+1}-\eta)^2-3(\eta_{i+1}-\eta)^3 & for \quad \eta_{i}\le\eta\le\eta_{i+1}\\ (\eta_{i+2}-\eta)^3 & for \quad \eta_{i+1}\le\eta\le\eta_{i+2}\\ 0 & otherwise\end{cases} \tag{3.9}$$

Here *h* denotes the distance between levels for regular spacing.

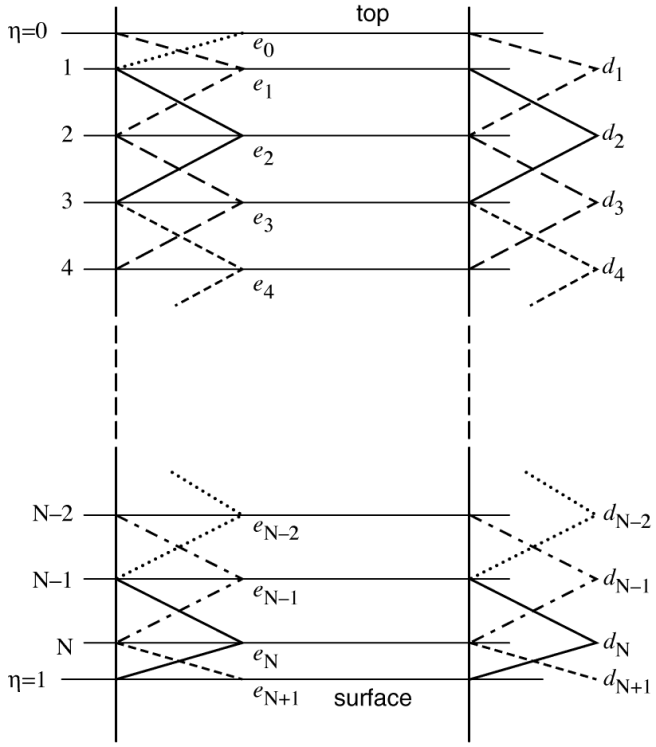

Fig. 1 Basis functions for the linear finite-element scheme: The set of hat functions on the left are used as basis functions for expanding the integrand and the set of functions on the right are the basis functions used for expanding the integral and as test functions. The horizontal lines numbered from 1 to N are the full model levels while the lines at $\eta=0$ *and* $\eta=1$ *indicate the top and the bottom of the atmosphere, respectively.*

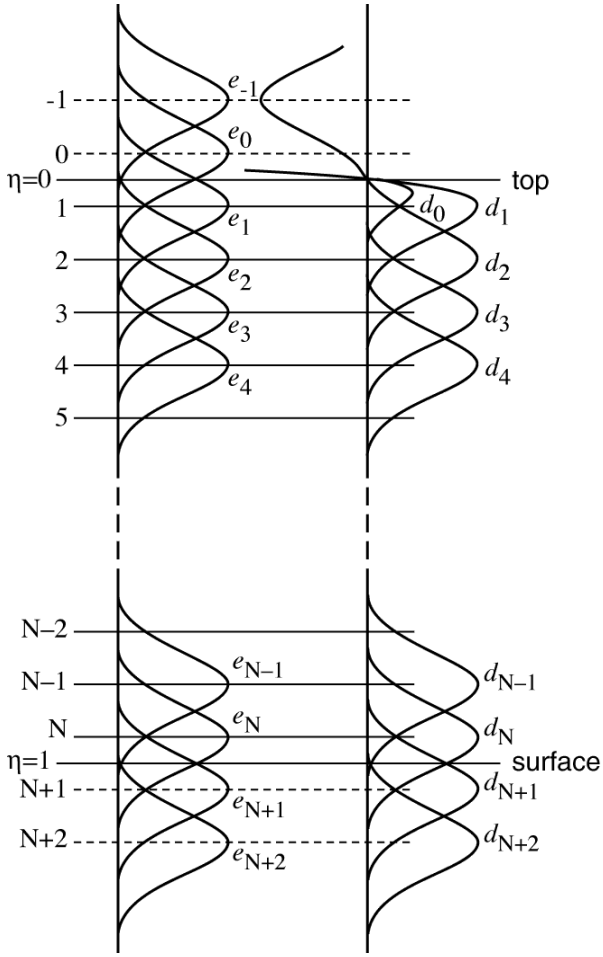

Fig. 2 Basis functions for the cubic finite-element scheme. The layout of this figure is as in Fig. 1 . The additional horizontal lines (dashed) above the top of the atmosphere and below the surface represent the levels at which the additional cubic B-splines, needed for a full coverage of the domain $\eta \in [0,1]$ *, are located.*

For a non-regular spacing of levels, the cubic B-splines can be constructed in a similar way from piecewise cubic polynomials with the conditions that they are twice continuously differentiable on the entire real line and that $B_i(\eta) \equiv 0$ *for* $\eta \le \eta_{i-2}$ *and* $\eta \ge \eta_{i+2}$, or by using the algorithm for generating B-splines given in *Prenter*, 1975, *section 4.3, pp 87*.

In order to cover the whole atmosphere with hat functions, *N*+2 linearly independent functions are needed, two more than the number of full model levels (one at each end of the atmosphere). This is necessary because the top and bottom full model levels do not coincide in our model with the top and the bottom of the atmosphere, respectively. With cubic B-splines four more functions than model levels are required, two at each end of the atmosphere, because each B-spline covers four intervals. These additional basis functions are chosen, in the linear case, to peak at the top ($\eta = 0$) and the bottom ($\eta = 1$) of the atmosphere , respectively, and thus having only about half the width of the other linear elements. In the cubic case we opted for a more uniform spacing of the additional nodes (levels) required above the first and below the last model level and located the additional basis functions centred at $-3\eta_1, -\eta_1, 1+(1-\eta_N)$ and at $1+3(1-\eta_N)$, i.e. outside the atmosphere.

In order to have sufficient conditions to determine the cubic spline interpolate of function f (i.e. the coefficients c_j in spline space), of which we know the values at the full model levels f_i, $1 \le i \le N$, we need also to specify values for f_{-1}, f_0, f_{N+1} and f_{N+2}, and for the first or the second derivatives of f at level -1 and at level N+2. We set $f_{-1} = f_0 = f_1$ and $f_{N+1} = f_{N+2} = f_N$, and specify the first derivatives of f as $f'_{-1} = 0$ and $f'_{N+2} = 0$. In the linear version it is sufficient to specify f_0 and f_{N+1}, and again we choose f_0=f_1 and f_{N+1}=f_N. The coefficients c_j can now be determined, in the cubic case, from the linear system of equations

$$\begin{cases} \sum_{i=-1}^{N+2} c_i e'_i(\eta_{-1}) = f'_{-1} \\ \sum_{i=-1}^{N+2} c_i e_i(\eta_j) = f_j \qquad \text{for } -1 \le j \le N+2 \\ \sum_{i=-1}^{N+2} c_i e'_i(\eta_{N+2}) = f'_{N+2} \end{cases} \tag{3.10}$$

which simplifies in the linear case to

$$\sum_{i=0}^{N+1} c_i e_i(\eta_j) = f_j \qquad 0 \le j \le N+1 \tag{3.11}$$

The solution written in vector form is $\vec{c} = \underline{\underline{S}}^{-1}\vec{f}$. Matrix $\underline{\underline{S}}^{-1}$ is the projection operator from physical space to finite-element space. Its existence is guaranteed for spline functions, because the matrix $\underline{\underline{S}}$ of system (3.10) is diagonally dominant. In the linear version, this projection operator is the unity matrix, since the hat functions are chosen to have the maximum value of 1 ($e_i(\eta_i) = 1$ for all $0 \le i \le N+1$) and they are zero at all other nodes ($e_i(\eta_j) = 0$ for $i \ne j$), i.e. the basis is an interpolatory basis unlike in the cubic case.

In both versions, linear and cubic, the set of test functions $\{t_j\}$ is chosen to be identical to the basis set for the integral $\{d_i\}$.

The basis functions in set $\{d_i\}$ are identical to those in set $\{e_i\}$ except for the functions extending into the first half layer (from the top of the atmosphere to the first full model level). These basis functions have been modified to be zero at the top of the atmosphere in order to ensure that the value of the integral at the top of the atmosphere, where the integration starts, is zero ($F(\eta = 0) \equiv 0$). For the linear elements it is straightforward to modify the topmost hat function to fulfil this condition. For the cubic elements three new, linearly independent, functions were constructed by linearly combining the B-spline located at node -1 (function e_{-1}) with those at nodes 0, 1, and 2, respectively, (i.e. e_0, e_1, and e_2) such that the new basis functions d_0, d_1, and d_2 are zero at the top of the atmosphere. Outside the atmosphere the new basis functions are negative, but this does not matter. Due to this "boundary" condition for the integral, the basis set $\{d_i\}$ has one function less than the set $\{e_i\}$.

The projection matrix $\underline{\underline{P}}$, whose inverse is required in the computation of matrix $\underline{\underline{I}}$, is obtained in the same way as matrix $\underline{\underline{S}}$ but using the basis set $\{d_i\}$ instead of the set $\{e_i\}$.

3.4 Accuracy of the finite-element integration

In order to check the accuracy of the derived linear and cubic FE integral operators and compare it to that of the FD scheme, we applied all three schemes to the integration of several smooth trial functions for which the analytical integral is known.

Table 1 shows as an example the results obtained for the function $\sin(6\pi x), x \in [0,1]$ at different resolutions N=60, N=90, N=120 and N=150, where N is the number of nodes positioned in the integration domain [0,1] at (n-1/2)/N, n=1,2,...,N to correspond to the positions of the full levels in our model for uniform spacing.

We compare the relative error (in %) with respect to the analytical solution of the integration over each inter-nodal interval for the FD scheme, the linear and cubic FE schemes and for the analytic integration of the cubic spline interpolate of the integrand (which we call cubic collocation scheme). The values given in Table 1 are averaged values over all inter-nodal intervals located within one wavelength of the integrand (the full wave located in the middle of the integration domain [0,1]).

As expected, the linear FE scheme is significantly more accurate than the FD scheme and the cubic FE scheme is again much more accurate than the linear FE scheme. From the values in Table 1, the order of convergence for the different schemes can be estimated. The result is given in the last row of the table. The FD scheme is second order accurate (as was to be expected for uniform spacing of the nodes), and for the linear and cubic FE schemes we obtain roughly order 4 and order 8, respectively. The cubic collocation scheme (which uses the same cubic basis functions to fit the integrand with a cubic spline as the cubic FE scheme) is only of 4th order accurate like the linear FE scheme.

Table 1

relative integration error [%]	**FD scheme**	**linear FE**	**cubic FE**	**cubic collocation**
N=60	0.82e+0	0.14e-2	0.90e-8	0.14e-2
N=90	0.37e+0	0.27e-3	0.32e-9	0.27e-3
N=120	0.21e+0	0.85e-4	0.31e-10	0.85e-4
N=150	0.13e+0	0.35e-4	0.55e-11	0.35e-4
estimated order of the scheme	2	4	8	4

Applying the Galerkin method in addition to a cubic spline fit of the integrand doubles the order of accuracy of the integration scheme (from 4 for the cubic collocation to 8 for the cubic FE). The same factor of 2 is obtained by going from linear collocation (which is identical to the FD scheme and therefore of second order) to the linear FE scheme. This suggests the following expression for the order of the FE integration scheme as a function of the degree k of the basis functions used for the scheme O(2(k+1)). This expression is in good agreement with error estimates derived in textbooks for FE approximations to the solution of differential equations (with sufficiently smooth right-hand sides) valid at the nodes (see for example *Oden*

and Reddy, 1976). In between the nodes the order is only k+1 according to the theory on finite elements (*Becker et al.*, 1981, *Oden and Reddy*, 1976), the same as for the collocation schemes. We did not test this for our schemes because the integration operators we have derived return by design only the integrals at the nodes. The accelerated convergence at the nodes with FE schemes is referred in the literature as super-convergence and is one reason for the superiority of the FE schemes over the collocation schemes.

4. Impact of the finite-element discretization on the forecast model

4.1 Impact on the linear vertical modes

A first impression on how changes to the vertical discretization affect the vertical structure of the model can be obtained by looking at the vertical modes of the linearized model. In the ECMWF model, the linear vertical modes are used in the semi-implicit time discretization, i.e. the implicit treatment of the linearized adjustment terms of the momentum, the thermodynamic, and the continuity equation. They are computed as follows.

The linearized form of the forecast equations (2.1) to (2.5) (linearized about an isothermal reference state at rest of constant temperature T_r and constant surface pressure $(p_s)_r$) can be written as (*Simmons and Burridge*, 1981; *Simmons and Temperton*, 1997)

$$\frac{\partial D}{\partial t} = -\nabla_H^2 \left[\gamma_r T + R_d T_r (\ln p_s) \right] \tag{4.1}$$

$$\frac{\partial T}{\partial t} = -\tau_r D \tag{4.2}$$

$$\frac{\partial}{\partial t}(\ln p_s) = -\nu_r D \tag{4.3}$$

where D is the horizontal divergence and greek letters indicate vertical operators, each depending on the reference state. These operators are defined as

$$(\gamma_r T)_\eta = -\int_1^\eta R_d T \frac{d}{d\eta'}(\ln p_r)\, d\eta' \tag{4.4}$$

$$(\tau_r D)_\eta = \kappa T_r \left(\frac{1}{p_r} \right)_\eta \int_0^\eta D \frac{dp_r}{d\eta'} d\eta' \tag{4.5}$$

$$\nu_r D = \frac{1}{(p_s)_r} \int_0^1 D \frac{dp_r}{d\eta} d\eta \tag{4.6}$$

Here p_r is the function defined by (3.1) for the finite difference scheme or by the vertical integral of (3.4) for the finite-element scheme, using as surface pressure the reference surface pressure $(p_s)_r$. In this study we use the same reference state of T_r = 350K and $(p_s)_r$ = 1000hPa that is used in the current operational semi-implicit semi-Lagrangian two-time-level scheme at ECMWF.

(4.1) to (4.3) can easily be combined into the following equation for divergence

$$\frac{\partial^2 D}{\partial t^2} - \nabla_H^2 \Gamma D = 0$$

where Γ is the vertical structure operator given by $\Gamma \equiv \gamma_r \tau_r + R_d T_r \nu_r$.

By expanding D in terms of eigenfunctions of the Laplace operator ∇_H^2, i.e. the spherical harmonics Y_n^m, we can write for each spectral component (n,m)

$$\frac{\partial^2}{\partial t^2} D_n^m(\eta,t) + \frac{n(n+1)}{a^2} \Gamma D_n^m(\eta,t) = 0 \qquad (4.7)$$

where *a* is the radius of the earth. In discretized form with N levels in the vertical, (4.7) represents a set of N equations coupled in the vertical by the matrix Γ. These equations can be decoupled by projecting onto the eigenspace of Γ. The eigenvectors of Γ are the linear vertical (gravity) eigenmodes and the corresponding eigenvalues are proportional to the square of the frequencies of the wave solutions of (4.7).

Matrix Γ combines all vertical integral types that have to be evaluated in the model, so changes to the numerical integration scheme should translate into differences in its eigenmodes, rendering them good test objects for assessing different vertical integration schemes.

We compare the eigenmodes of Γ obtained numerically with the FE integration schemes (linear and cubic) to those obtained with the Simmons & Burridge FD scheme in Lorenz arrangement of variables (FD_Lorenz scheme) and also to the eigenmodes computed with FD in Charney-Phillips arrangement (*Charney and Phillips*, 1953) (FD_Charney-Phillips scheme), where the horizontal winds and the temperature are held at different sets of levels (the winds at full levels and the temperature at half levels).

Fig. 3 shows the eigenvalues of matrix Γ as a function of mode number obtained with these four integration schemes at two different vertical resolutions using 50 and 100 levels, respectively. The spacing of the levels is equidistant in ln(p) and the top full level is located at 0.1hPa. As reference we use the eigenvalues computed with 1000 levels. At this high resolution the four integration schemes have converged well over the range of eigenmodes plotted in this figure and the four curves are virtually indistinguishable.

For coarser vertical resolutions, the eigenvalues obtained with the FD_Lorenz scheme are smaller than the reference values, i.e. the waves have too small phase speeds and lag behind the reference solution. The error is increasing rapidly towards the end of the spectrum. In Charney-Phillips arrangement, the eigenvalues are larger than the reference values, i.e. the waves are too fast, but the error is smaller than with the Lorenz staggering and does not show accelerated growth at the end of the spectrum (see also *Beland et al*.,1983).

The eigenvalues obtained with the two FE schemes are smaller than the reference values and the curves have a similar shape to the FD_Lorenz curve, but the errors are very much smaller. For the cubic FE scheme, the first 70 modes out of 100 (in the 100-level resolution) have an error of less than 1%. For the linear FE scheme the first 47 modes have this level of error, while this is true only for the first 13 modes for the FD_Lorenz scheme and for 17 modes for the FD scheme in Charney-Phillips arrangement. In the 50-level resolution the number of eigenvalues with a relative error of less than 1% are 35 for the cubic and 24 for the linear FE scheme, only 7 for the FD_Lorenz scheme and 8 for the FD_Charney-Phillips scheme, giving very similar percent values (i.e. $100N_{<1\%}/N$, where N is the total number of modes) as for the 100-level resolution.

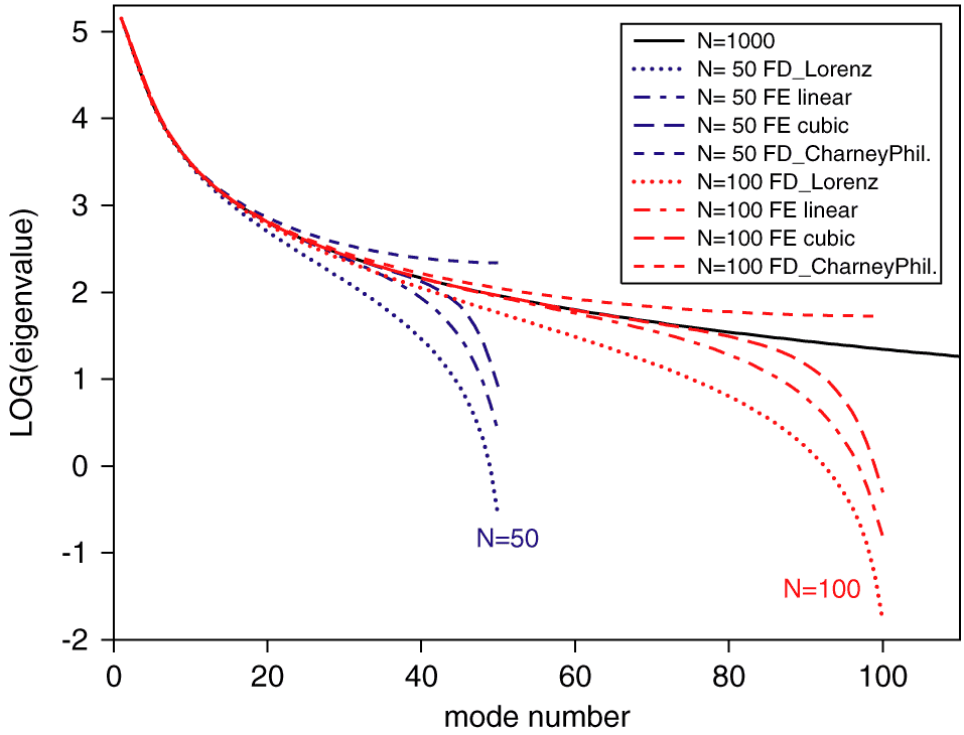

Fig. 3 Eigenvalues of the vertical structure matrix for the linearized divergence equation as a function of eigenvector number, using an uniform distribution of levels in terms of ln(p). Full (black) line is obtained with 1000 levels and is used as reference. Dotted lines show the result obtained with the finite-difference scheme in Lorenz staggering, short-dashed with the finite-difference scheme in the Charney-Phillips staggering, dash-dot line with the linear finite-element scheme and long-dashed with the cubic finite-element scheme. Blue lines are for a resolution with 50 levels and red lines with 100 levels.

We tested several resolutions between 50 and 200 levels and found that the percentage of modes with errors less than 1% is remarkably independent on vertical resolution for all four schemes. The average values are, 70% for the cubic and 47% for the linear FE scheme, but only 13% for the FD_Lorenz scheme and 17% for the FD_Charney-Phillips schemes. The improvement of 34 percentage points brought about by the linear FE scheme over the FD scheme is impressive, and is due to the application of the Galerkin method in constructing the FE integral operator. Using cubic instead of linear elements leads to a further improvement by 23 percentage points.

Fig. 3 also shows that an impressive 43 modes out of 50 computed with the cubic FE scheme at the 50-level resolution have smaller errors than the corresponding modes obtained at twice this resolution with the FD_Lorenz scheme. For the linear FE scheme this is true for the first 34 modes. Compared with the FD_Charney-Phillips scheme at 100-level resolution, the first 41 modes out of 50 have smaller error for the cubic and 29 for the linear FE scheme at only half the resolution.

At the tail of the spectrum, the error with the FE schemes is quite large (larger than with the FD_Charney-Phillips scheme for the last 3 modes of the cubic FE scheme at N=50 and 7 at N=100) but significantly smaller than with the FD_Lorenz scheme.

The spacing of levels in the vertical resolution currently operational at ECMWF for the analysis- forecast system (L60) is not equidistant in ln(p) as in these tests. Near the surface the layer thickness is as small as 20m and increases gradually throughout the troposphere and lower stratosphere to reach 1.5km near 50hPa.

It is kept constant at this value to about 5hPa and then grows again towards the top of the model. The distribution of these 60 levels is shown in Fig. 4. (If not specifically stated otherwise, the numerical experiments discussed in this paper were run at this vertical resolution.)

Fig. 5 shows the eigenvalues of the matrix Γ as a function of mode number for this L60 resolution, obtained with the four numerical schemes discussed above. Included is also the curve of eigenvalues computed with the cubic collocation scheme. It is almost identical to the curve for the linear FE scheme. This is not surprising since the integration errors we found with the convergence tests described in sect. 3.4 are very similar for the two schemes (see Table 1). With this non-uniform spacing of levels in the L60-distribution, the shape of the eigenvalue curve obtained with the FD_Charney-Phillips scheme differs substantially for large mode numbers from that obtained with regular spacing in ln(p) and is now more similar to the shape of the FD_Lorenz curve. The eigenvalues at the end of the spectrum decrease rapidly, as is the case also for the FD_Lorenz scheme, but stay more than an order of magnitude larger than those of the FD_Lorenz scheme. The kink in the FD_Charney-Phillips curve at around mode 32 is linked to the equidistant spacing of levels in height between 50hPa and 5hPa in L60. The eigenvalues computed with the two FE schemes are again significantly larger than the FD_Lorenz eigenvalues. The smallest eigenvalue for the cubic FE scheme is roughly an order of magnitude larger than the smallest FD_Lorenz eigenvalue. For the case of the linear FE scheme it is larger by about a factor of 4. This increase in the smallest eigenvalues with the cubic FE scheme together with the decrease in amplitude of the grid-wave oscillations in the eigenfunctions of Γ discussed below, proved to be important for making data assimilation experiments, run with the ECMWF 4D-Var system using potential vorticity as a control variable (where operator Γ needs to be inverted), to work (*Cullen*, 2002).

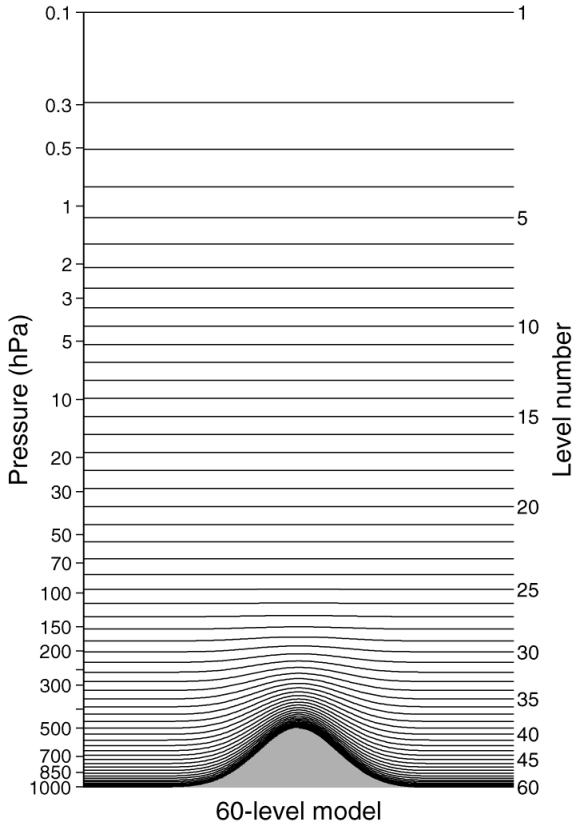

Fig. 4 Distribution of the hybrid levels in the operational 60-level version of the ECMWF forecast model.

The most striking difference in the eigenvectors of matrix computed with the different integration schemes at L60 occurs in the upper part of the model (stratosphere) for eigenvectors corresponding to medium and small eigenvalues (i.e. for mode numbers from 35 to about 55). The eigenvectors computed with the FD scheme in Lorenz arrangement have large amplitude oscillations of $2\Delta\eta$-character while the corresponding eigenvectors obtained with the FD scheme in Charney-Phillips arrangement are almost zero at these levels and have significant amplitude only in the lower part of the model (at levels with large level numbers). The eigenvectors computed with the FE schemes have $2\Delta\eta$-oscillations of significantly smaller amplitude than the FD_Lorenz eigenvectors. The cubic FE scheme reduces these oscillations more than the linear scheme. Fig. 6a illustrates this for eigenvector number 40 and Fig. 6b for eigenvector number 50.

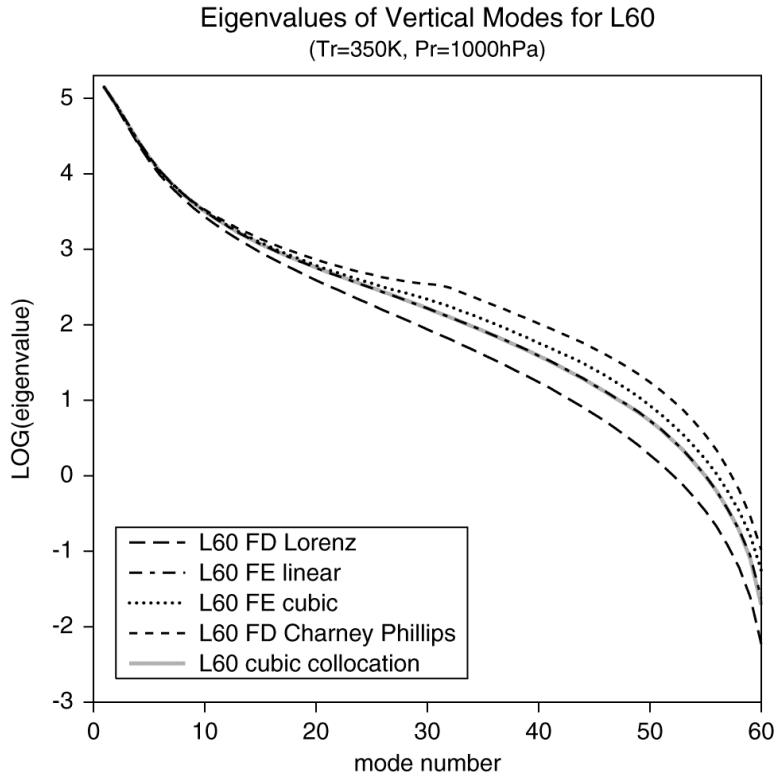

Fig. 5 Eigenvalues of the vertical structure matrix for the linearized divergence equation as a function of eigenvector number using the 60 levels of Fig. 4. The dotted line was obtained with the cubic finite-element scheme, dash-dotted line with the linear finite-element scheme, thin full line (on top of the dash-dotted line) with the cubic collocation method, long-dashed line with the finite-difference scheme in Lorenz staggering and short-dashed with finite-differences in the Charney-Phillips staggering.

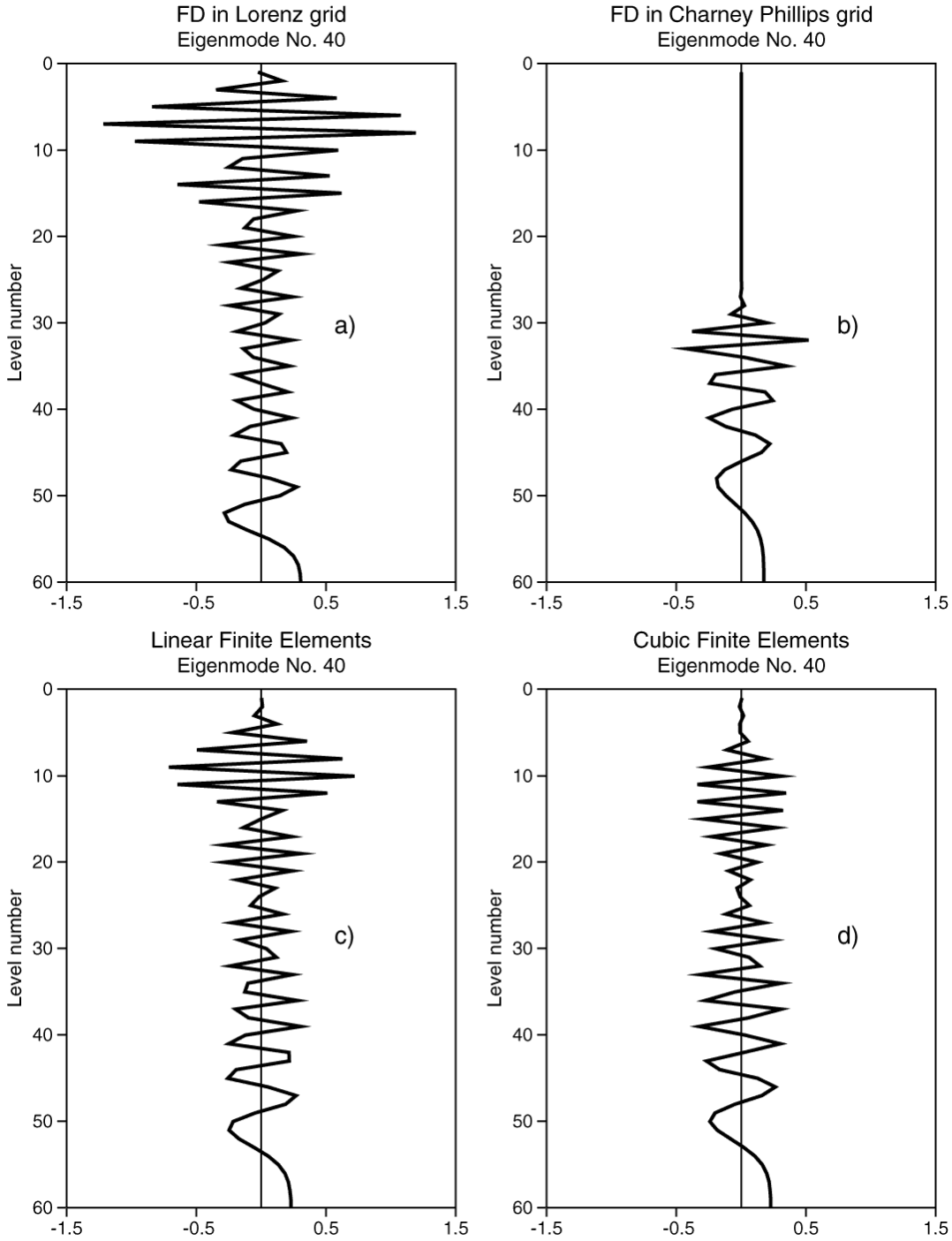

Fig. 6a Structure of eigenmode No. 40 of the vertical structure matrix Γ for the 60-level model computed with finite-differences in Lorenz (a) and in Charney-Phillips (b) arrangements and with the linear (c) and cubic (d) finite-element schemes.

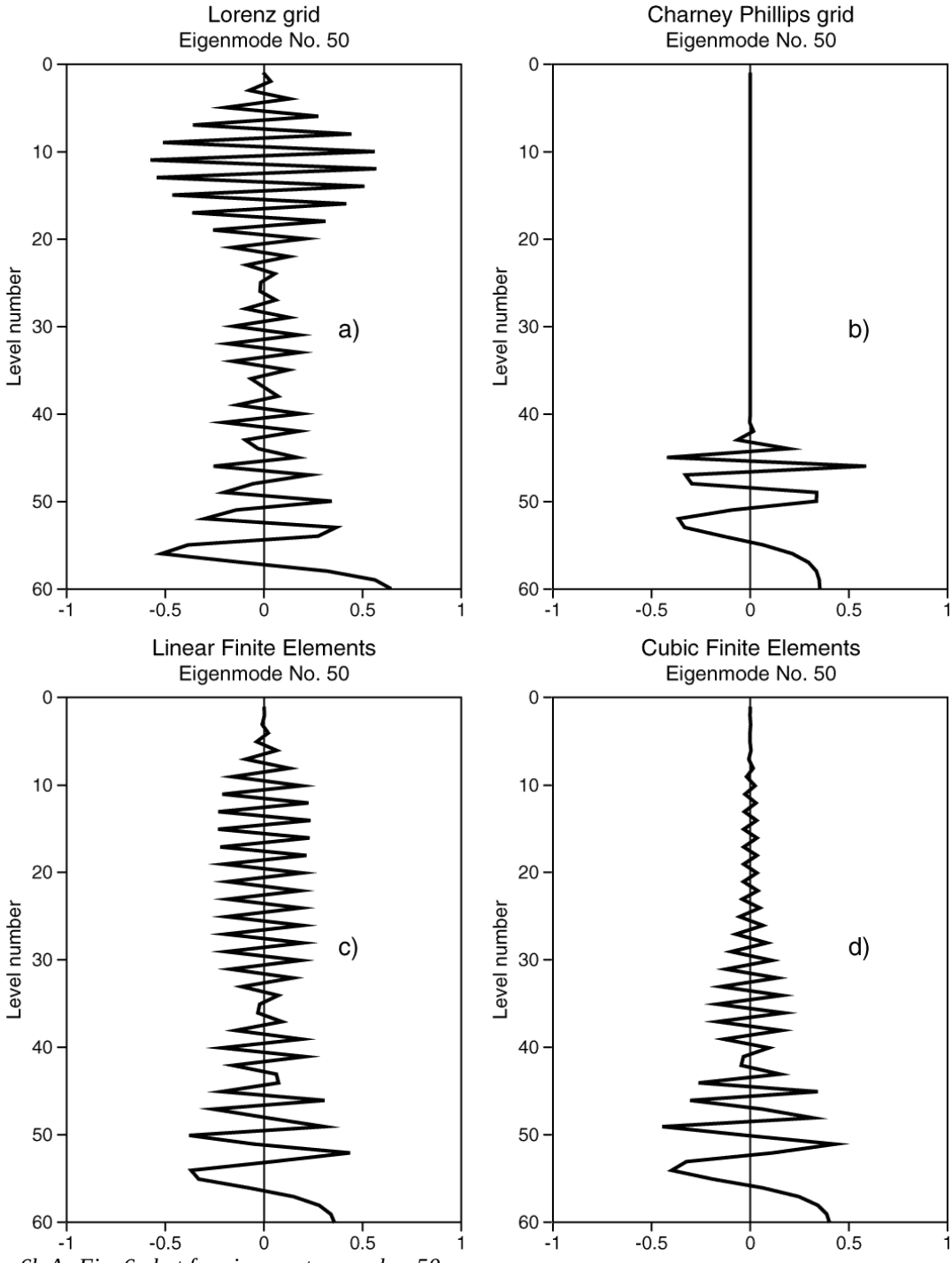

Fig. 6b As Fig. 6a but for eigenvector number 50.

We believe that these large amplitude $2\Delta\eta$-oscillations in the eigenvectors of the FD_Lorenz scheme are linked to the existence of a computational grid-wave mode with Lorenz staggering (*Hollingsworth*, 1995, *Arakawa and Konor*, 1996) which is absent with Charney-Phillips staggering. Certainly, they are an undesirable feature since they are at the limit of the vertical resolution and can only be regarded as vertical noise. Therefore, a numerical scheme that reduces the amplitude of these oscillations is to be preferred.

Judging by the results obtained with the different integration schemes for the linearized model, we expect the non-linear model integrated with the FE schemes to be less susceptible to the excitation of large amplitude $2\Delta\eta$-waves than the FD_Lorenz scheme. To test this, we have performed a simple numerical experiment with the non-linear dynamical core of the ECMWF model where we tried to excite a vertical grid-wave structure in the temperature field by diabatic heating at only one level and looked at the response of the model with the FD_Lorenz scheme and with the linear and the cubic FE schemes. Unfortunately, we do not have a non-linear model with Charney-Phillips staggering of variables available for this test as well. This experiment is similar in design and setup to one of the experiments used by *Arakawa and Konor* (1996) to demonstrate the existence of the computational mode in the Lorenz grid. We started from an isothermal atmosphere of 250K at rest and integrated the dynamical core (no tendencies from physical parametrizations) of the non-linear model at resolution T_L95L60 with flat orography using semi-Lagrangian time discretization with a timestep of 1h. At level 40 (~540hPa) we added at each timestep a temperature tendency of $+0.01K/24h \cdot \sin\lambda\cos\theta$, where λ denotes longitude and θ latitude.

Fig. 7 shows vertical profiles of temperature at 0°N and 90°E obtained with the three discretization schemes at the end of the run (after 14400h of integration). In the upper part of the model, the temperature profiles for the different schemes are resembling to some degree the vertical structure of their eigenvectors (see Fig. 6b). Correspondingly, the vertical grid oscillations are greatly reduced with the two FE schemes, mainly with the cubic version. This is an indication that the spurious mode in Lorenz arrangement can be damped with FE schemes (or maybe even eliminated if high order elements are used).

The two FE schemes are also reducing the amplitude of $2\Delta\eta$-oscillations in vertical profiles of divergence, often seen in the tropical stratosphere in forecasts run with the full model (with physical parametrizations switched on) using the FD_Lorenz scheme. In order to quantify this visual impression somewhat, we computed the Fourier decomposition of vertical profiles of divergence (as a function of level number) over the top 24 levels of L60 (i.e. above 100hPa) and averaged over the deep tropics (from 10°N to 10°S). Fig. 8 shows "spectra" computed in this way for 3-day forecasts, run with the FD_Lorenz scheme, with the linear and with the cubic FE schemes, together with the spectrum of the analysis from which these forecasts were started. For the analysis the FD_Lorenz scheme was used. After 3 days, the cubic FE scheme has reduced the amplitude of the $2\Delta\eta$ structure (wave number 12) and other poorly resolved vertical structures by almost 1/3, while there is only a very small decrease with the FD_Lorenz scheme. The similarity in the level of vertical noise (i.e. poorly resolved vertical structures) in the stratospheric analysis and forecasts suggests that it is a feature of the model numerics and not forced in by the assimilated data. Assimilations using the FE schemes have a reduced level of vertical noise in the stratosphere (not shown). The linear FE scheme reduces the poorly resolved structures slightly more than the cubic FE scheme, but damps the somewhat better resolved structures too much.

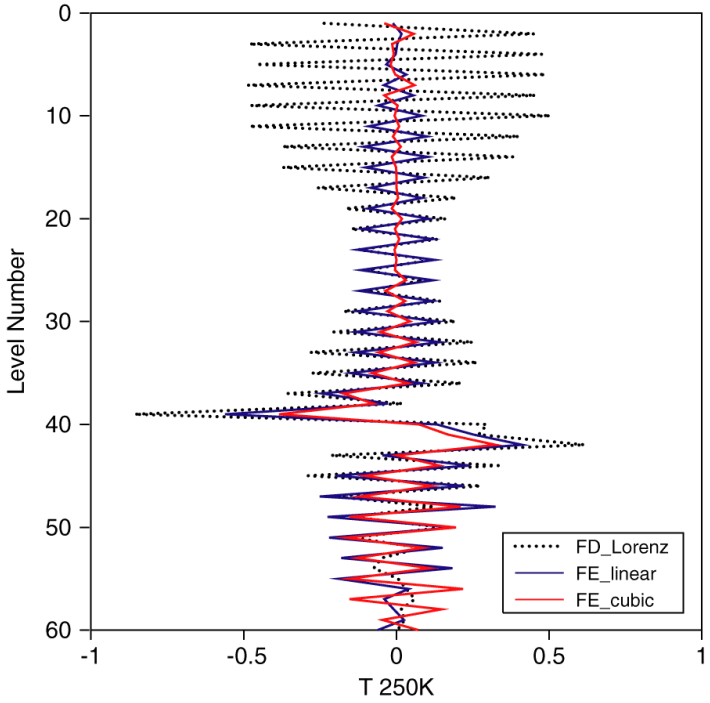

Fig. 7 Vertical profiles of temperature at 0^oN and 90^oE obtained with the finite-difference (FD) scheme in Lorenz staggering (black dotted line), with the linear finite-element (FE) scheme (blue full line) and with the cubic finite-element scheme (red dashed line) in a dynamical core experiment with heating at only one level to excite the computational mode of the Lorenz grid. See text for more details.

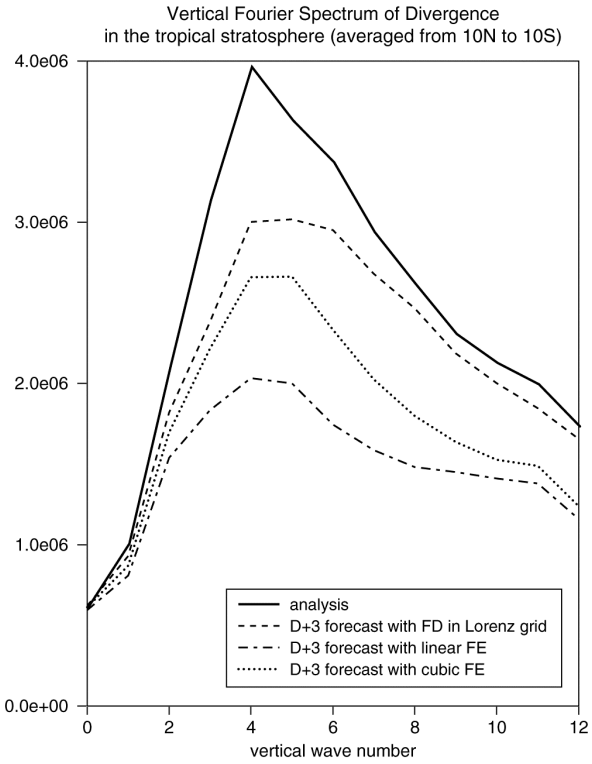

Fig. 8 Fourier decomposition of vertical profiles of divergence (as a function of level number) over the top 24 levels (i.e. above 100hPa) averaged over the deep tropics (from 10^oN to 10^oS). The solid line is the spectrum of the analysis from which forecasts with the finite-difference (FD) scheme in Lorenz arrangement, with the linear finite-element scheme (linear FE) and with the cubic finite-element scheme (cubic FE) were started. The broken lines show the spectra at day 3 of the forecast as indicated in the legend.

4.2 Impact of the cubic finite-element scheme in assimilation-forecast experiments

Extended periods of data assimilation with the 4-dimensional variational method (4D-Var) have been run using the cubic FE scheme in the forecast model as well as in the tangent linear and adjoint model. From the analyses corresponding to 12Z, 10-day forecasts were run. The results are compared to control experiments using the (then operational) FD scheme in the Lorenz grid. Fig. 9 compares the fit of first guess and analysis to TEMP temperature observations, averaged over 62 assimilation cycles, from the FE experiment and the control FD experiment. The number of observations accepted into the analysis is larger in the FE experiment at most levels, with the largest differences (of 0.5-3%) in the tropical stratosphere. Also, the bias and the standard deviation of the difference between the first guess and the observations are markedly reduced in the stratosphere in the FE experiment compared to the control in spite of more observations having been accepted into the analysis (first guess and analysis are compared only to the accepted observation not to all available observations). Fig. 9 shows results for a winter period (January 2001); very similar results have been obtained also for the summer period (not shown). The improved fit of the first guess to observations at stratospheric levels in the FE experiments is partly due to the reduction of vertical noise in the stratosphere with the FE scheme and partly to a reduction in the cold bias in the first guess of the lower stratosphere present with the FD scheme.

The main impact of the FE discretization on the 10-day forecast is also found in the stratosphere. A substantial reduction of RMSE for temperature is found in the lower stratosphere at all forecast ranges and all verification areas, with the largest improvement occurring in the tropics.

Fig. 10 compares mean temperature verification scores (anomaly correlation and RMSE) at 50 hPa in the northern hemisphere (NH), tropics and southern hemisphere (SH) from 10-day forecasts run with the cubic FE scheme and with the FD scheme (control). The average is over 98 forecasts (67 summer cases and 31 winter cases). All forecasts were started from analyses run with the same vertical discretization as the forecasts. They are also verified against their corresponding analyses. The improvements in temperature RMSE at this level are very consistent (high statistical significance levels) as is shown in the corresponding scatter diagrams presented in Fig. 11. The large reduction in the value of RMSE with the FE scheme is largely due to a marked reduction in the cold bias present with the FD scheme in the lower stratosphere. The evolution of the mean error in temperature during 10-day forecasts at 50hPa is shown in the right-hand side column of Fig. 10. In the NH and in the tropics the cold bias of the FD scheme is roughly halved by the cubic FE scheme and in the SH it is reduced to about 1/3. Wind scores in the stratosphere are also improved (not shown). In the troposphere the impact of the FE scheme on the verification scores is neutral (not shown) except in the upper troposphere in the tropics (at 200 and 100hPa), where the existing positive temperature bias with the FD scheme is made slightly worse by the FE scheme.

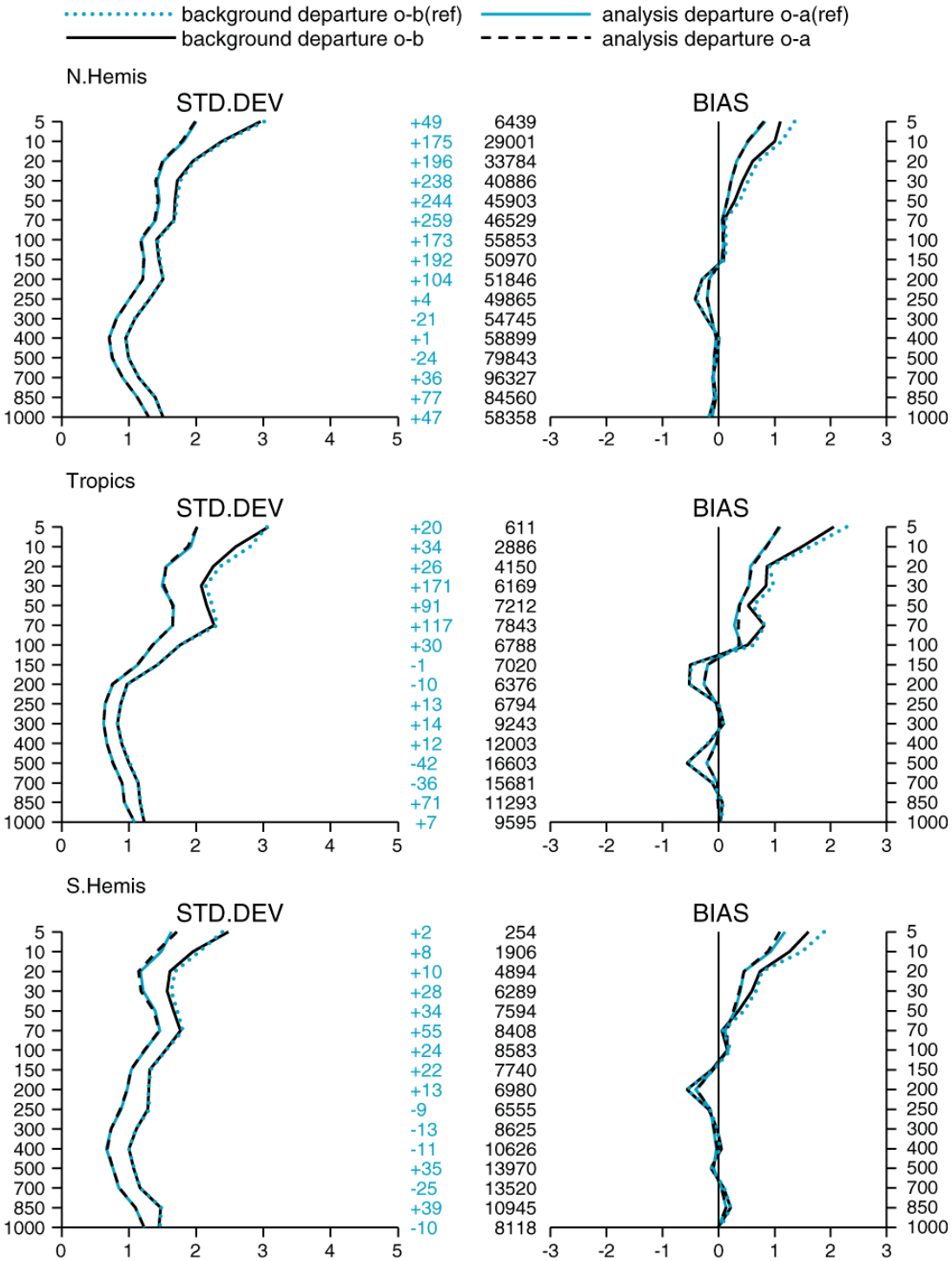

Fig. 9 Fit of temperature TEMP observations to the first guess (full line) and to the analysis (broken line) averaged over 62 assimilation cycles for an assimilation experiment using the cubic finite-element scheme (black lines) as compared with the control experiment (red) which uses finite-differences in the Lorenz grid. The numbers in black show the total number of observations used while those in red give the difference with respect to the control experiment (positive means more observations have been used in the FE experiment than in the FD control run).

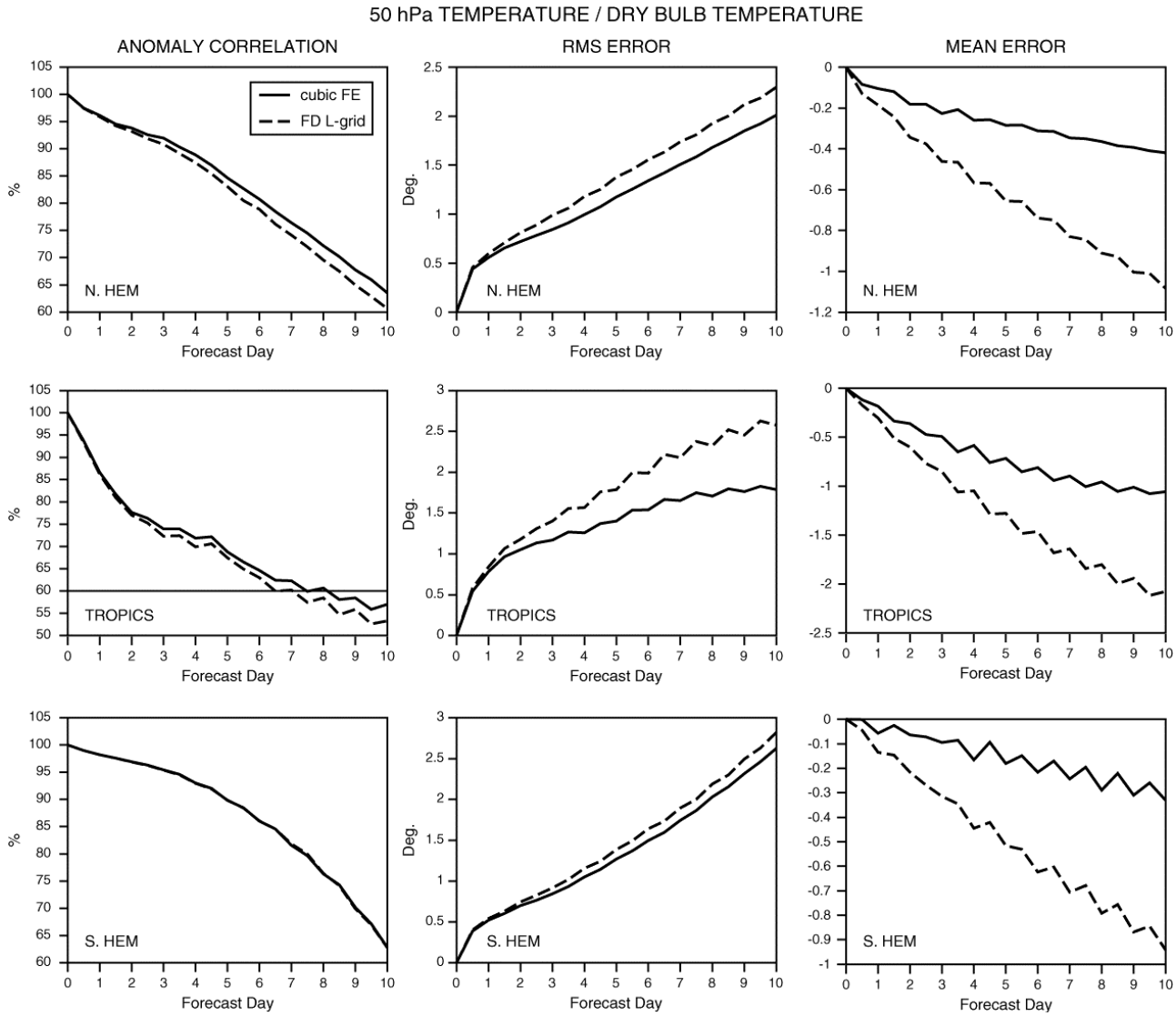

Fig. 10 Mean Temperature verification scores at 50 hPa for 98 10-day forecasts (67 summer cases and 31 winter cases) with the cubic finite-element (FE) scheme (solid line) compared with the control experiments using finite-differences in the Lorenz grid (FD L-grid) (dashed line). The left-hand side column shows anomaly correlation, the middle column root mean square error and the right-hand side column shows the bias (mean error). Top figures are for northern hemisphere, middle figures for tropics and the lower figures for southern hemisphere.

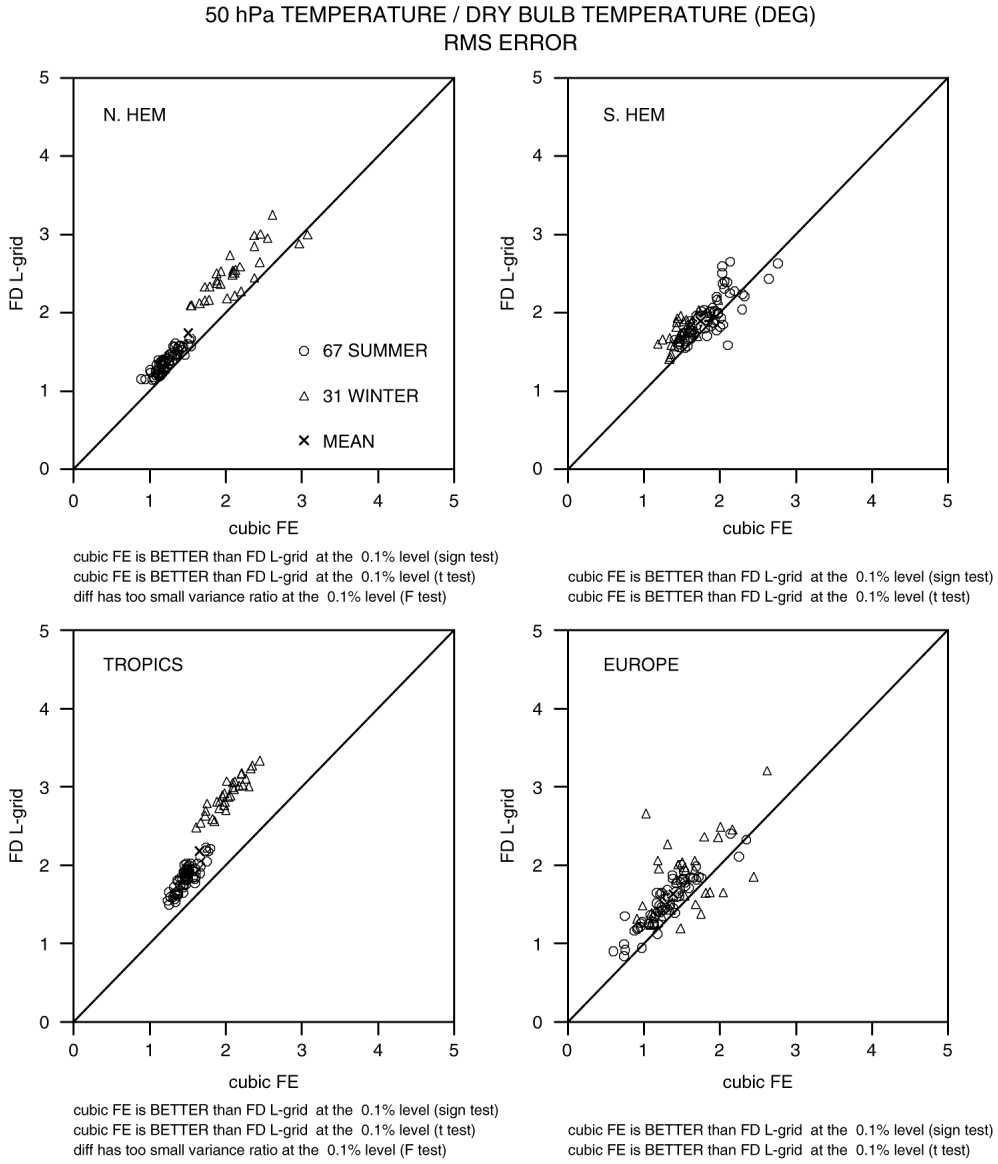

Fig. 11 Scatter diagrams comparing RMSE of temperature at 50hPa for the same 98 forecasts as in Fig. 10. The different panels show different verification areas. Clockwise from top left: N-hemisphere, S-hemisphere, Europe, and tropics. At the bottom of each panel, information about the statistical significance of the difference between the two sets of experiments is given.

The improvements in the stratosphere with the FE scheme translate into a better conservation of ozone, as shown in Fig. 12. The semi-Lagrangian advection scheme used in the ECMWF model does not conserve tracers by construction and about 4% of the global mass of ozone is lost on average over 60 days of integration (with the ozone chemistry parameterization switched off) when using the FD scheme.

The two main sources for this ozone loss are errors in the advective wind field (mainly in the vertical wind) and errors in the interpolation of the ozone field at the departure point of the semi-Lagrangian trajectory (again mainly in the vertical interpolation). With the FE scheme the ozone loss is reduced by about 50%. This is due to a better vertical transport in the stratosphere (mainly to a slower upward movement in the tropics), resulting from an improved computation of the vertical integral in the expression for the vertical velocity $\dot{\eta}$, (2.11). The remaining ozone loss can be reduced further substantially by using cubic spline

interpolation for the vertical interpolation of ozone at the departure point instead of 4-point Lagrange interpolation used here (not shown).

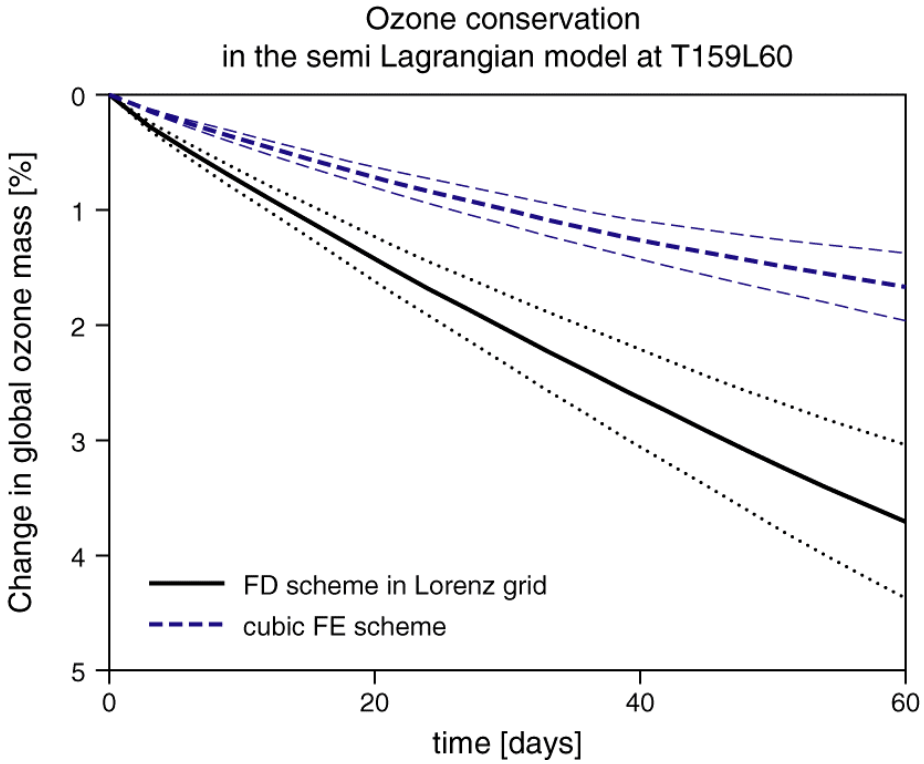

Fig. 12 Conservation of ozone in the semi-Lagrangian model: Plotted is the change in % in global ozone mass during 60-day forecasts at using the FD scheme in Lorenz arrangement (solid line) and the cubic FE scheme (dashed line). The thick lines are the means over 24 forecasts (2 for each month) and the thin lines indicate the spread ($mean \pm stdev$ *).*

5. Summary and discussion

We have presented a finite-element discretization scheme for the vertical of the ECMWF model designed to be used in conjunction with semi-Lagrangian advection. Only non-local vertical operations are performed in FE space, products of dependent variables are evaluated in physical space ("transform method"). Since the only non-local vertical operations in the semi-Lagrangian version of the ECMWF model are vertical integrations, the FE discretization involved only the derivation of an integration operator in FE representation. We used the Galerkin method and B-splines as basis functions with compact support and derived two versions of the integration operator, a linear version based on piecewise linear functions and a cubic version based on cubic B-splines. In both versions, the integration operator is a full matrix and operates directly on the integrand given on the model levels and returns the integral from the top of the model to each level and to the surface, i.e. the transformations from physical space to FE space and back are incorporated into the integration matrix and not performed explicitly, as is the case with the spectral transform method used for the horizontal.

Since the integration matrix is a full matrix for both the cubic as well as the linear FE scheme, the computational cost of applying these two schemes is the same (save for a small extra cost for the cubic scheme in the initialisation phase), i.e. it is independent of the degree of the B-splines used as basis

functions. For a 10-day forecast with the full model the cost of the FE scheme is 3% higher than with the FD scheme.

No staggering of dependent variables is used in this vertical discretization to avoid the difficulties staggering causes for semi-Lagrangian advection, in that it requires the winds and all the advected variables to be given

at the same levels. However, keeping the geopotential and the temperature at the same levels (Lorenz staggering) can lead to a large amplitude vertical "zigzag" mode in the temperature field ("computational mode") (*Arakawa and Konor*, 1996). The FE schemes described here reduce the amplitude of this mode in temperature considerably (the cubic scheme much more than the linear) as has been demonstrated in section 4.1. By using Charney-Phillips staggering in the vertical, this computational mode can be suppressed completely (*Arakawa and Konor*, 1996), but at the price of having to interpolate the temperature field to the levels where the winds are held (or vice versa) for semi-Lagrangian advection. This interpolation can introduce errors if not done carefully and adds to the computational cost. The cubic FE scheme makes a very good compromise between the convenience of the Lorenz grid with semi-Lagrangian advection and the nice property of the Charney-Phillips grid of being free of the computational mode in temperature, present with the Lorenz grid.

The linear FE integration is 4th order accurate on the nodes away from the upper and lower boundaries and the cubic is of order 8 when used for integrating smooth functions. This high accuracy in evaluating integrals translates into a much improved accuracy in the phase speeds of the linear gravity waves obtained with the FE schemes compared with the FD schemes.

Due to the much higher accuracy at almost no additional cost of the cubic FE scheme compared to the linear scheme, the cubic version has been chosen for implementation into the operational version of the ECMWF model and it has been tested extensively in assimilation-forecast experiments. The main benefits from the cubic FE scheme are a reduction of the persistent cold bias in the lower stratosphere (by about 50% at 50hPa) and a marked reduction in vertical noise in the stratosphere. Both improvements (reduction in cold bias and vertical noise) lead to a better fit of the first guess fields to observations in the lower stratosphere (mainly for temperature TEMP data) and to more observations being accepted into the analysis. They also lead to a significant improvement in the lower stratospheric verification scores, with the largest improvement found in temperature in the tropics, but wind scores are also improved. Tropospheric scores are neutral except at 200hPa and at 100hPa in the tropics, where the FE scheme slightly worsens an existing warm bias.

The FE scheme also improves the vertical transport in the lower stratosphere and around the tropopause, leading to better conservation of ozone. The loss in global ozone mass of almost 4% in 60-day forecasts with the FD scheme at T_L159L60 is halved by the cubic FE scheme.

Based on these positive results, the cubic FE scheme became operational at ECMWF on 22 January 2002 in all the configurations (deterministic forecast mode, variational assimilation mode, ensemble forecast mode) which are run using the semi-Lagrangian advection scheme. It is also being used in the 40-year reanalysis project (ERA40).

Acknowledgment The authors are grateful to A. Hollingsworth, M. Miller and A. Staniforth for helpful comments and suggestions to improve the manuscript.

6. References

Arakawa, A., and C. S. Konor, 1996: Vertical differencing of the primitive equations based on the Charney-Phillips grid in hybrid vertical coordinates. *Mon. Wea. Rev*., **124**, 511-528

Becker, E. B., G. F. Carey and J. T. Oden, 1981: FINITE ELEMENTS, An Introduction, Volume I. *Prentice-Hall, Inc., Englewood Cliffs, New Jersey 07632*.

Beland, M., J. Cote and A. Staniforth, 1983: The accuracy of a finite-element vertical discretization scheme for primitive equation models: Comparison with a finite-difference scheme. *Mon. Wea. Rev*., **111**, 2298-2318

Burridge, D. M., J. Steppeler and R. Strüffing, 1986: Finite element schemes for the vertical discretization of the ECMWF Forecast Model using linear elements. *ECMWF Technical Report No. **54***.

Charney, J. G., and N. A. Phillips, 1953: Numerical integration of the quasi-geostrophic equations for barotropic and simple baroclinic flows. *J. Meteor*., **10**, 71-99.

Cullen, M. J. P., 2002: Use of potential vorticity as a control variable within a 4D variational data assimilation system. *ECMWF Technical Memorandum 358*.

Francis, P. E., 1972: The possible use of Laguerre polynomials for representing the vertical structure of numerical models of the atmosphere. *Quart. J. Roy. Meteor. Soc.*, **98**, 662-667.

Hollingsworth, A., 1995: A spurious mode in the "Lorenz" arrangement of and T which does not exist in the "Charney-Phillips" arrangement. *ECMWF Technical Memorandum*, No. 211.

Hoskins, B., 1973: Comments on "The possible use of Laguerre polynomials for representing the vertical structure of numerical models of the atmosphere" by P. E. Francis. *Quart. J. Roy. Meteor. Soc.*, **99**, 571-572.

Lorenz, E. N., 1960: Energy and numerical weather prediction. *Tellus*, **12**, 364-373.

Oden J. T.,and J. N. Reddy, 1976: An introduction to the mathematical theory of finite elements, *John Wiley& Sons*. ISBN 0-471-65261-X.

Prenter, P. M., 1975: Splines and variational methods, *John Wiley& Sons*. ISBN 0-471-69660-9.

Ritchie H., C. Temperton, A. J. Simmons, M. Hortal, T. Davies, D. Dent and M. Hamrud, 1995: Implementation of the semi-Lagrangian method in a high-resolution version of the ECMWF forecast model, *Mon. Wea. Rev*. **123**, No 2, 489-514.

Simmons A. J., and D. M. Burridge, 1981: An energy and angular momentum conserving vertical finite difference scheme and hybrid vertical coordinates. *Mon. Wea. Rev*. **109**, 758-766.

Simmons A. J., and C. Temperton, 1997: Stability of a two-time-level semi-implicit integration scheme for gravity wave motion. *Mon. Wea. Rev*. **125**, 600-615.

Simmons A. J., and R. Strüfing, 1983: Numerical forecasts of stratospheric warming events using a model with hybrid vertical coordinate. *Quart. J. Roy. Meteor. Soc.*, **109**, 81-111.

Staniforth, A. N., and R. W. Daley, 1977: A finite-element formulation for the vertical discretization of sigma-coordinate primitive equation models. *Mon. Wea. Rev.* **105**, 1108-1118.

Steppeler, J., 1986: Finite elements scheme for the vertical discretization of the ECMWF Forecast Model using quadratic and cubic elements. *ECMWF Technical Report No.* ***55***.

Steppeler, J., 1987: Quadratic Galerkin finite element schemes for the vertical discretization of numerical models. *Mon. Wea. Rev.* **115**, 1575-1588.

Tokioka, T., 1978: Some considerations on vertical differencing. *Meteor. Soc. Japan*, **56**, 89-111.